Chemical Physics 539 (2020) 110927

Contents lists available at ScienceDirect

Chemical Physics

journal homepage: www.elsevier.com/locate/chemphys

Solvation of HeH^+ in neon atoms: Proton-bound complexes of mixed He and Ne

Jax Dallas[a], Athena Flint[b], Ryan C. Fortenberry[a,*]

[a] Department of Chemistry & Biochemistry, University of Mississippi, University, MS 38677-1848, United States
[b] Department of Chemistry, Yale University, New Haven, CT 06520, United States

ARTICLE INFO

Keywords:
Noble gas molecules
Quantum chemistry
Proton-bound complexes
Astrochemistry

ABSTRACT

The proton-bound complexes of the structure Ne_xHeH^+, with x ranging from one to four, are explored to investigate the effect of additional neon atoms on binding energies and bright vibrational modes of complexes involving HeH^+. The first chemistry that occurred within the universe took place between helium and hydrogen, producing HeH^+, which has been shown to solvate successfully with neon to form $NeHeH^+$. CCSD(T)/aug-cc-pVTZ computations show that additional neon atoms in the complex are bound more loosely but still destabilize the existing He–H bond. Additionally, as more neon atoms are added, the harmonic frequencies of the species begin to converge to approximately 1580 cm^{-1}, roughly 60 cm^{-1} less than the $NeHeH^+$ proton-bound complex. Neon destabilizes the HeH^+ structure in every instance, no matter the amount of neons added or whether additional heliums are added.

1. Introduction

Chemists have long had conflicts about how noble gases fit into the puzzle of the study of matter. Noble gases are often labeled as nothing more than ornaments to adorn the rightmost edge of the periodic table and placeholders for the completion of the various orbital shells. They are lauded for their inertness, but their chemistry is far from dull [1–7]. In fact, helium, the lightest noble gas, and hydrogen were actually the first element to engage in chemistry in the early universe. After the age of electron–ion recombination, helium atoms bonded with protons that were yet to undergo recombination themselves [8,9]. This association is fundamental to the eventual formation of the H_3^+ ion, a molecule that acts as a "hydrogen factory" for the subsequent gas-phase formation of small molecules that then seeded the chemical universe [10,11]. Without this reaction between He and H^+, the steps to form H_3^+ would not have been able to outpace the rapid expansion of the universe, and everything chemical we know would never have come to pass. This reasoning places HeH^+ at the root of all chemistry, and information collected from further studies of this molecule can transform the way that the early universe is understood.

Studies of this molecule have only been encouraged by the recent discovery of HeH^+ in the NGC 7027 nebula by Güsten et al. [12]. While this region for observation is not the edge of the universe, where primordial HeH^+ would be detected (and has yet to be) [13], its presence provides a natural environment where this molecule's chemistry can be directly observed [14]. This molecule can be examined here on Earth and actually has been since its first observation in 1925 [15]. However, the high reactivity of HeH^+ prevents traditional approaches to exploring its chemistry from being readily applied. A recent cryogenic ion storage ring experiment by Novotný et al. [16] investigates recombination rates for different electronic states of HeH^+ which provides new estimates for its likely higher primordial abundance. However, the large, expensive equipment used in experiments like this one is not easily accessible and hinders the study of this and related noble gas molecules.

An alternative approach to the study of transient molecules such as noble gas species is matrix isolation spectroscopy. Matrix isolation avoids setbacks attributed to the difficulties of studying both gas-phase and transient molecules via the entrapment of the species in question within a solid [17,18]. The lightweight noble gases (He, Ne, and Ar), when sufficiently cooled, are often used for this purpose due to the spectroscopic clarity that they provide and their typical lack of reactivity with the species to be observed. Despite these precautions, HeH^+ is so reactive that the proton will, at best, likely be shared among the solvating host atoms, as well [19,20]. This is due to the exceedingly low proton affinity of helium. Hence, at best, matrix isolation experiments will only produce proton-bound complexes of helium either with other helium atoms or the matrix gas, likely neon or argon. Proton-bound complexes of HeH^+ with other noble gases have been studied extensively recently [21–24] even solvated within other helium atoms

* Corresponding author.
E-mail address: r410@olemiss.edu (R.C. Fortenberry).

https://doi.org/10.1016/j.chemphys.2020.110927
Received 10 June 2020; Received in revised form 10 July 2020; Accepted 12 July 2020
Available online 25 July 2020
0301-0104/

[25,26], but how HeH^+ behaves when solvated in more than one non–helium noble gas atom has yet to be seen [27,23]. Knowledge of such behavior would help to understand what the limits are to the stability of this first molecule in the universe.

The $HeHHe^+$, $HeHNe^+$, and $NeHNe^+$ noble gas, proton-bound molecules have similar bond strengths, force/spring constants, and bonding behavior. For instance, the He–H and Ne–H force constants change by less than 5% between $HeHHe^+$ and $HeHNe^+$ [23]. The inclusion of argon changes the bonding environments notably. The larger and more polarizable argon atom preferentially binds to the proton, leaving the He or Ne atom weakly bound in a van der Waals-type complex for $ArHHe^+$ and $ArHNe^+$ [22,23]. Clearly, inclusion of one neon atom with HeH^+ does not do this [23], but can two or more? He and Ne are among the five most abundant elements in the universe [28] making associations of these atoms possible in various astronomical environments. Furthermore, such mixed species could play a role in other proton-bound complexes with molecules that also have "ideal gas" properties like CO or N_2 [29–33].

Proton-bound complexes are characterized by their exceptionally bright infrared features for the motion of the central proton between the two exterior ligands. Most of the charge is moving with the proton, while most often single-digits percentages of the mass are moving at the same time. This produces extreme intensities with the infrared, with the anharmonic frequency of the proton shuttling motion occurring at 1453.6 cm^{-1} for $NeHeH^+$ [23]. The frequencies will shift based on the bonding character of the proton-bound complex [21–23,29] and the presence of any potential distant ligands, but the large peak is indicative of a proton-bound complex making them relatively easy to detect in the infrared even if they are somewhat metastable.

As a result, the present study examines the structures, binding energies, and vibrational frequency shifts of the Ne_xH^+ ($x = 1 - 5$), Ne_xHeH^+ ($x = 1 - 4$), and $Ne_4He_2H^+$ proton-bound families. While Ne matrix isolation of HeH^+ is almost certainly impossible, this quantum chemical study will provide insights into how HeH^+ would behave in a Ne matrix or with Ne tagging. Quantum chemistry is flexible enough and, with current methods, accurate enough to provide insights into such systems where stand-alone experiments are exceedingly challenging. While NeH^+ will likely not be observed in astrophysical regions due to an unfavorable potential energy surface (PES) [34,35], the role that neon atoms could play in the degradation of HeH^+ in regions like NGC 7027 where it is known to exist will be explored here. Furthermore, the manner in which neon atoms likely usurp the strongest bonding positions of the helium atoms in such proton-bound complexes will be provided. These insights may provide laboratory scientists with more data such that, at least, proton-bound complexes of $HeHNe^+$ could be observed in matrix isolation potentially increasing the natural inventory of noble gas molecules.

2. Computational details

Initial geometry optimizations of molecular formulas Ne_xH^+ ($x = 1 - 5$), Ne_xHeH^+ ($x = 1 - 4$), and $Ne_4He_2H^+$ utilize restricted Hartree–Fock reference wave functions and coupled cluster singles, doubles, and perturbative triples (CCSD(T)) along with the aug-cc-pVTZ basis set within the MOLPRO 2015.1 quantum chemistry program [36–43]. Basis set superposition error (BSSE) was not considered, as previous work with noble gas atoms has shown that BSSE is unlikely to be large enough to affect conclusions [44]. Following these, harmonic vibrational frequency calculations are carried out to determine the zero-point vibrational energies of the optimized molecules. The frequency calculations also confirm that the molecule in question is a minimum on its potential energy surface. Additionally, MP2/6–31 + G(d) computations within Gaussian09 provide the intensities for the double-harmonic vibrational frequencies [45–47] shown to be in good agreement with higher-level, anharmonic intensities for $NNHNN^+$ [31]. Sequential binding energies (BEs) for Ne_xH^+ (neon) and Ne_xHeH^+ (mixed neon and helium) are calculated using the following formulae:

$$BE(He) = E(Ne_xHeH^+) - E(Ne_xH^+) - E(He) \quad (1)$$

and

$$BE(Ne) = E(Ne_xHeH^+) - E(Ne_{x-1}HeH^+) - E(Ne). \quad (2)$$

The binding energy of the distant neon is found by allowing the $Ne_{x-1}HeH^+$ structure to optimize freely. The binding energy of the close helium atom is determined by constraining the geometrical parameters to those of the minimum save for the He–H bond length. The same procedure is employed for the neon energies as well. In the previously-examined, proton-bound, noble gas complexes, the binding energy drops notably when $n \geqslant 7$ implying a filled first solvation/complexation shell after six atoms surround the proton [21,25]. Hence, this study will not move beyond this limit of six atoms in addition to the proton. The BEs are reported as negative, showing that the bound complexes are more favorable than the lone atoms.At each optimized geometry the harmonic vibrational frequencies are computed, and the resulting zero-point vibrational energies are added to the electronic energies for the reported, relative and binding energy values.

A relaxed PES scan is also performed for the lowest-energy constitutional isomers of Ne_xHeH^+ ($x = 1 - 4$) and $Ne_4He_2H^+$. The HeH^+ bond length is fixed for each point in the scan, and the rest of the molecule is allowed to optimize. Each new computation changes the HeH^+ bond distance by a length of 0.05 Bohr. The ground-state electronic energies of these optimized geometries are collected and plotted as a function of the HeH^+ bond length in order to provide a meaningful interpretation of each PES.

3. Results & discussion

3.1. $NeHeH^+$

Table 1 provides the binding energy and structural parameters for $NeHeH^+$. Previously, this molecule was called $HeHNe^+$, but it will be referred to from here on as $NeHeH^+$ in order to remain consistent with the present Ne_xHeH^+ family nomenclature where $x = 1$ in this case. The Ne BE is within 3.0 kcal/mol and He BE within 0.5 kcal/mol of previous CCSD(T)/aug-cc-pV5Z benchmarks [23]. The destabilization effect that neon atoms have on the He binding energy is seen through the change in the binding energy of the close He as the number of neons in the Ne_xHeH^+ species increases. This is the difference in the close He BE of the species in question and that of the $x = 1$ species. This value is given in subsequent tables as Δ close He BE.

The bond lengths of $NeHeH^+$ are within 0.02 Å of even higher-level theory where complete basis set extrapolations, core electron correlation, and scalar relativity (CcCR) are included [23]. The present 1641.3 cm^{-1} harmonic frequency in Table 1 is around 70 cm^{-1} higher than the CcCR value at 1569.8 cm^{-1}. The CcCR anharmonic value from the same, previous study is 1453.6 cm^{-1}, and CcCR has been shown to produce anharmonic vibrational frequencies regularly within 5 cm^{-1} and often within 1 cm^{-1} of gas phase experiment [48–56,22,57]. While

Table 1
Optimized properties of NeHeH+.

close Neon BE (kcal/mol)	17.11
close Helium BE (kcal/mol)	10.23
ω_1 (cm^{-1})	1641.3
ν_1 (cm^{-1})	1453.6[a]
scale	0.8856
f_1 (km/mol)	2617
H–Ne Bond Length (Å)	1.111
H–He Bond Length (Å)	0.953

[a]Ref. [23].

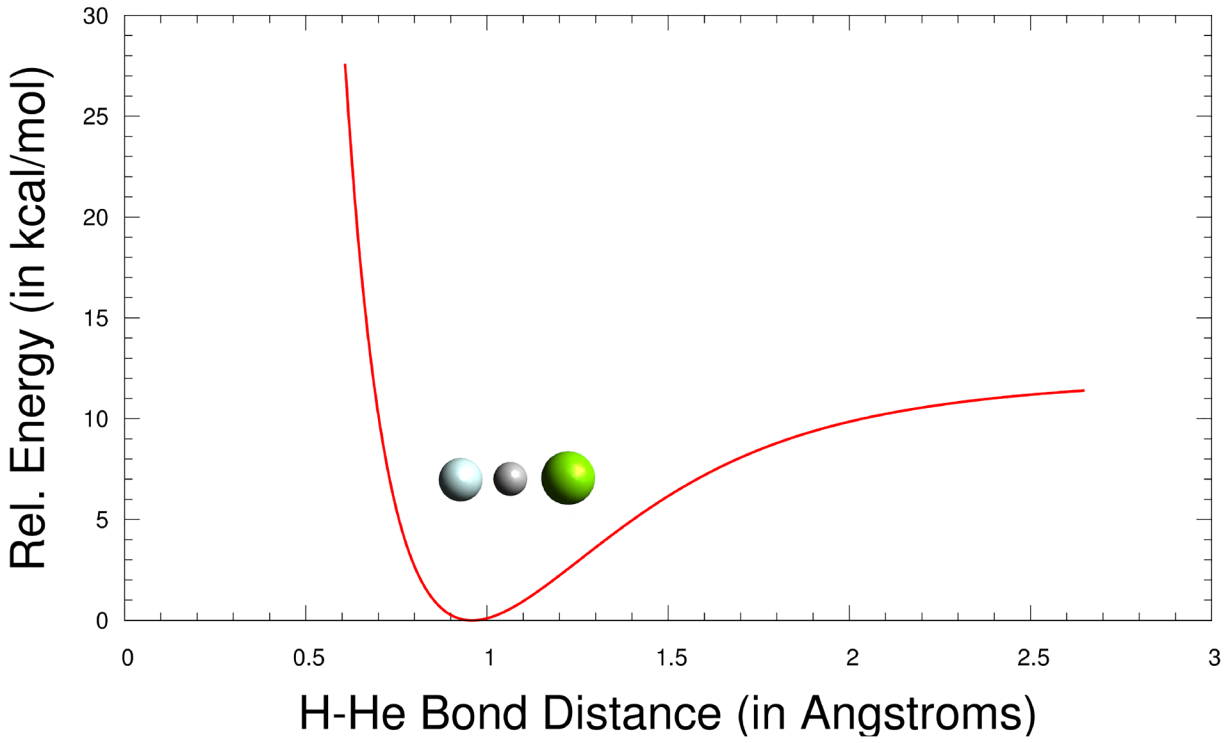

Fig. 1. The He–H dissociation PES for $NeHeH^+$ with the minimum energy structure shown.

there is some discrepancy between the present CCSD(T)/aug-cc-pVTZ results and those from earlier work, on the whole, the present computations demonstrate solid performance. Such higher-level computations are not feasible for the higher x values in this Ne_xHeH^+ family, implying that CCSD(T)/aug-cc-pVTZ should be adequate for analysis of the larger complexes in this family. Likely, this value of 1463.6 cm^{-1} is higher than the actual, physical value since previous CcCR values for He_2H^+ and Ar_2H^+ have been higher than their corresponding experimental frequencies [23,26,22,21]. However, the shifts brought about by higher numbers of neon atoms should remain physically relevant.

Fig. 1 shows the PES scan for elongating the He–H bond length; clear Morse behavior is present. The larger, bright green atom is the Ne, while the smaller, light blue one is He. The He is well-bound if only at 10.23 kcal/mol. As evident in Table 1 the Ne is around 50% more tightly bound, but the helium atom will not spontaneously leave the system, as is shown in Fig. 1. In either case, the bright proton shuttle frequency (ω_1) is well below the He BE implying that it will be visible if this molecule could form.

The brightest vibrational frequency, noted as ω_1 or ν_1 depending upon whether reported as harmonic or anharmonic, respectively, will be the most important observable for this study. The full set of harmonic vibrational frequencies for this and the other molecules in this study are given in the Supplemental Information (SI). From Table 1, the f_1 intensity is 2617 km/mol; For comparison, the notable antisymmetric stretch in water at this same level of theory is ~ 70 km/mol. This antisymmetric stretching frequency has such a tremendous intensity resulting from nearly all of the charge but very little of the mass moving as the proton shuttles between the two heavier atoms. The shift in ω_1 between higher x values or isomers of a given x level will be scaled in order to provide a good estimate for how the vibrational frequency will change upon isomerization or addition of further Ne atoms. The ratio of ν_1/ω_1 for $NeHeH^+$, as given in Table 1, is 0.8856, and the raw shift in the harmonic frequencies relative to the $x = 1$ species [$\Delta(\omega_1)$] will be multiplied by this value creating $\Delta(\nu_1)$. The resulting shift [$\Delta(\nu_1)$] will be added to the 1453.6 cm^{-1} CcCR anharmonic frequency [23] in order to provide an estimate for the new complex's anharmonic vibrational frequency. For Ne_2H^+, the CCSD(T)/aug-cc-pVTZ harmonic frequency is 1616.2 cm^{-1}, and the anharmonic CcCR value is 1436.6 cm^{-1} [22]. The ratio for the $NeHNe^+$ moiety will then be 0.8889. Hence, this $\Delta(\nu_1)$ will be the applied to ν_1 for $NeHeH^+$ or Ne_2H^+ depending upon the isomer in question. These shifts will clearly show the progression of neon coordination around the central proton and allow for any potential experimental corroboration.

3.2. Ne_2HeH^+

In moving on to $x = 2$ for the Ne_xHeH^+ family, Ne_2HeH^+ in this case, there are two isomers. The one with the helium atom more closely bonded to the proton is listed as structure a. The one with the Ne–H–Ne moiety and the helium atom noncovalently bonded (with the helium BE of 1.20 kcal/mol) is structure b. in Fig. 2. Structure b. is the lowest-energy isomer by 4.48 kcal/mol from Table 2, and this is given visually in Fig. 2. Once the He–H bond length surpasses 1.3 Å in structure a., the PES takes on the form of structure b. with the bond angles changing. There is a near minimum on the red, structure b. He–H PES nearly at the minimum for the blue structure b. in Fig. 2, but the triligated proton-bound complex is ultimately not favored. The optimized parameters of the two structures are given in Table 2 showing clear noncovalent interactions in the long bond lengths of one Ne atom in structure a. and the He atom in structure b. (See Table 3).

Even in structure a. where the Ne–H–He moiety is maintained, the helium is somewhat less well bonded in the presence of the second neon atom. As seen by Δ close He BE in Table 2 the close helium BE drops relative to $NeHeH^+$ by a mere 0.39 kcal/mol to 9.84 kcal/mol. However, the distant neon BE in structure b. is also much less than in $NeHeH^+$ implying that the noble gas atoms are perturbing one another and competing with one another. Additionally, this behavior was also shown with $ArHHe^+$ and $ArHNe^+$ [22,23], but, presently, this is not influenced by the stronger Ar–H bond. Hence, the weakening of the He–H and Ne–H bonds in these proton-bound complexes appears to arise more from more competition for interactions with the proton than from the type of atom producing the competition.

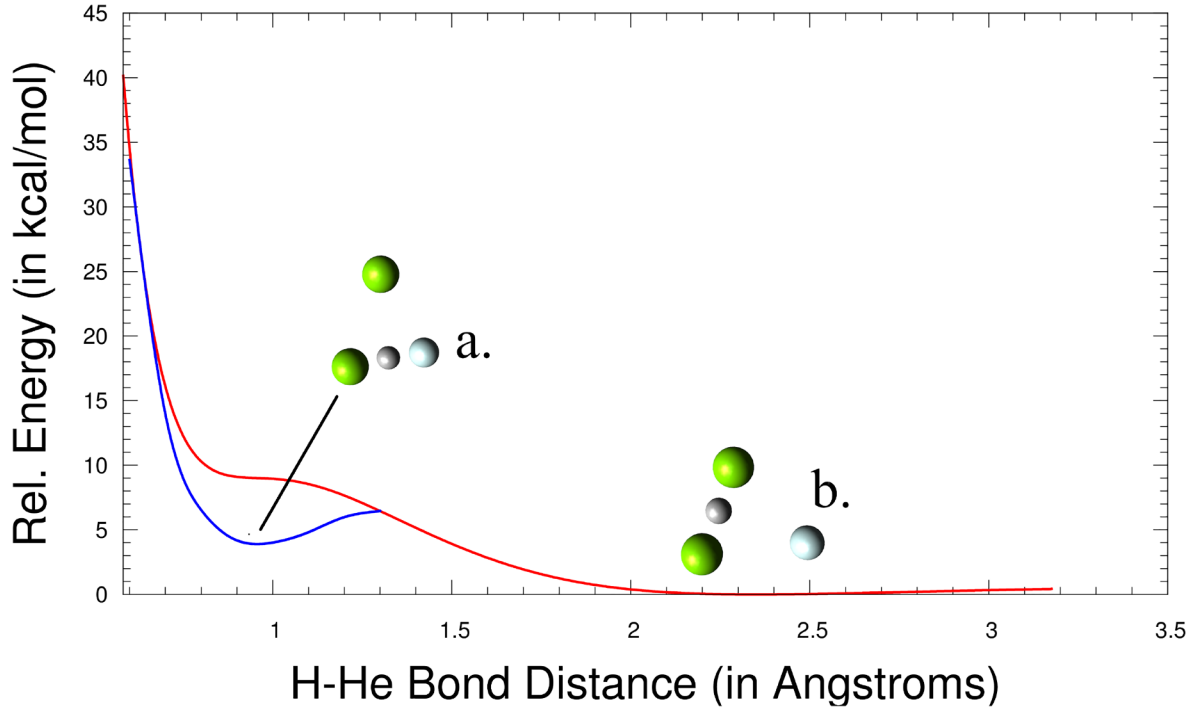

Fig. 2. The He–H dissociation PES for the two isomers of Ne_2HeH^+: Structure a. in blue and b. in red.

Table 2
Optimized properties of Ne_2HeH+.

	Structure a.	Structure b.
ΔE (kcal/mol)	4.48	0.00
distant Ne BE (kcal/mol)	1.35	5.84
distant He BE (kcal/mol)	–	0.57
close Ne BE (kcal/mol)	16.69	15.25
close He BE (kcal/mol)	9.84	–
Δ close He BE (kcal/mol)	−0.39	–
ω_1 (cm^{-1})	1620.3	1607.8
$\Delta(\omega_1)$ (cm^{-1})	−21.0	−33.5
$\Delta(\nu_1)$ (cm^{-1})	−18.7	−29.7
f_1 (km/mol)	2199	2468
H–He Bond Length (Å)	0.900	2.200
H–Ne_1 Bond Length (Å)	1.144	1.140
H–Ne_2 Bond Length (Å)	2.347	1.141

Table 3
Optimized properties of Ne_3HeH+.

	Structure a.	Structure c.
ΔE (kcal/mol)	4.29	0.00
distant Ne BE (kcal/mol)	1.47	1.27
distant He BE (kcal/mol)	–	0.62
close Ne BE (kcal/mol)	16.29	14.95
close He BE (kcal/mol)	9.24	–
Δ close HE BE (kcal/mol)	−0.99	–
ω_1	1588.4	1588.2
$\Delta(\omega_1)$ (cm^{-1})	−52.9	−53.1
$\Delta(\nu_1)$ (cm^{-1})	−46.8	−47.2
f_1 (km/mol)	2103	2371
H–He Bond Length (Å)	0.979	2.434
H–$Ne_{1/2}$ Bond Length (Å)	2.334	1.141
H–Ne_3 Bond Length (Å)	1.103	2.439

Regardless, each of these structures will have a unique ν_1 allowing for characterization. The $\Delta(\omega_1)$ for structure a. relative to $NeHeH^+$ actually is negative at -21.0^{-1} since the additional neon atom increases the harmonic frequency. This puts $\Delta(\nu_1)$ at $-18.7\,cm^{-1}$ and the likely ν_1 at $1434.9\,cm^{-1}$. For structure b. inclusion of the helium atom expectedly lowers the harmonic frequency to $1607.8\,cm^{-1}$ producing the $\Delta(\omega_1)$ of $-33.5\,cm^{-1}$ and $\Delta(\nu_1)$ of $-29.7\,cm^{-1}$. Consequently, the signature antisymmetric stretch of Ne_2HeH^+ will be $-29.7\,cm^{-1}$ lower in frequency than the Ne_2H^+ at close to $1420.1\,cm^{-1}$.

3.3. Ne_3HeH^+ & Ne_4HeH^+

The Ne_3HeH^+ PES in Fig. 3 is quite similar to that for Ne_2HeH^+ in Fig. 2. The blue line leading to the minimum structure (structure c.) has its minimum with the Ne–H–Ne moiety. This blue line, again, has a near-minimum above the red line's minimum (structure a.) where the proton-bound complex has a Ne–H–He moiety. The red line is allowed to continue in this plot to give a third stationary point on the PES in structure b. However, structure b. is actually not a true minimum as it gives an imaginary frequency in an a″ mode. The breaking of the symmetry allows the molecule to rearrange into structure c. Consequently, removing the imaginary portion of the red He–H PES produces a plot nearly identical to that from Ne_2HeH^+ in Fig. 2. Hence, more global behavior for HeH^+ solvated in neon atoms in the Ne_xHeH^+ family appears to be surfacing even for $x = 3$.

The addition of the neon atom will lower the ν_1 frequency notably compared to the lone $NeHeH^+$ molecule; $\Delta(\nu_1)$ is $-46.8\,cm^{-1}$. Expectedly, the bright frequency will red-shift as more neon atoms are added. This is borne out in structure c. where a neon atom is now part of the noncovalent shell along with the helium atom. However, this shift in Ne_2H^+ is not nearly as great compared to that from $NeHeH^+$. Furthermore, the addition of the neon atom further destabilizes the He–H bond, leading to a decrease in -0.99 kcal/mol for the close He BE from NeHeH.

Fig. 4 highlights the same behavior for Ne_4HeH^+ as is shown for Ne_2HeH^+ and Ne_3HeH^+. The additional neon atom is too far removed from the proton for there to be any notable, qualitative effect in the PES. This is further corroborated by the structural, BE, and vibrational

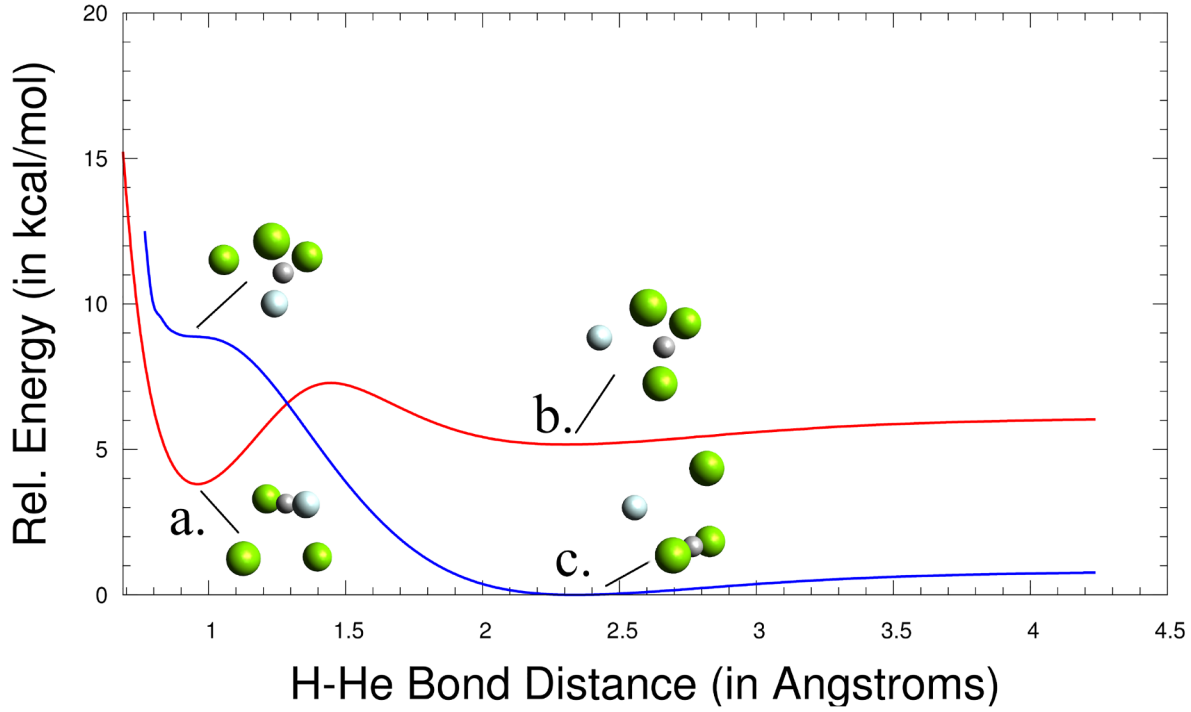

Fig. 3. The He–H dissociation PES for the two isomers of Ne_3HeH^+: Structure a. in blue and c. in red.

frequency data in Table 4. The BEs and frequencies show a minimal decrease for Ne_4HeH^+ relative to Ne_3HeH^+ implying a notable level of convergence. This is further confirmed in Fig. 5 which shows that as more neons are added to the Ne_xHeH^+ species the harmonic frequencies begin to converge. While Ne_7HeH^+ will likely have a marked drop in Ne BE compared to the $x = 6$ complex from previous work [21,25], the Ne atoms are bound to this proton more strongly than argon (~ 2.2 kcal/mol) and helium (~ 1.0 kcal/mol) in proton-bound complexes and clusters containg only one type of noble gas atom.

The harmonic vibrational frequency for Ne_4HeH^+ structure a. in Table 4 appears to settle around 1578.9 cm^{-1} putting the estimated anharmonic value at 1398.3 cm^{-1}. For the structure with the Ne–H–Ne moiety (structure b.), the anharmoinc frequency appears to converge to close to 1581.2 cm^{-1} harmonically and 1400.2 cm^{-1} anharmonically. However, the barrier to isomerization is less than 3.0 kcal/mol (1050 cm^{-1}) making observation of the bright, antisymmetric ν_1 difficult for He–H–Ne bearing structure a. While Feshbach resonances or other means of observing the vibrational frequency above the PES

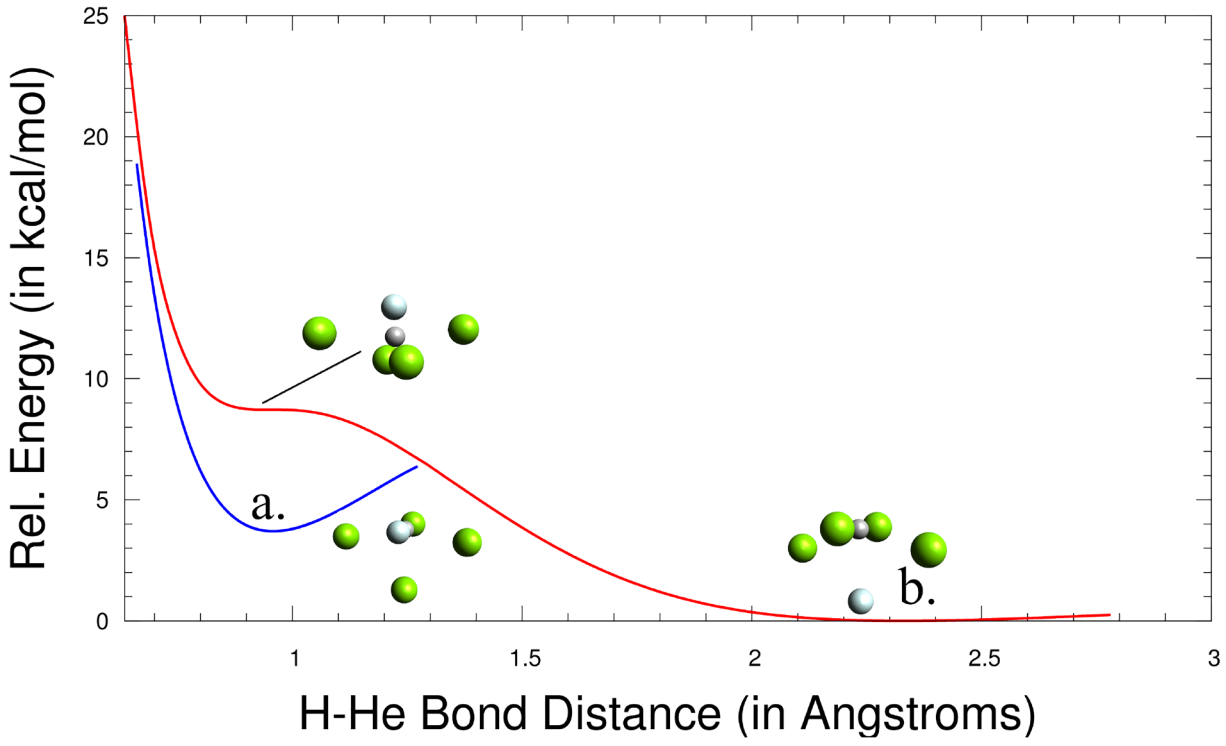

Fig. 4. The He–H dissociation PES for the two isomers of Ne_4HeH^+: Structure a. in blue and b. in red.

Table 4
Optimized properties of Ne_4HeH+.

	Structure a.	Structure b.
ΔE (kcal/mol)	4.25	0.00
distant Ne BE (kcal/mol)	1.42	1.38
distant He BE (kcal/mol)	–	2.90
close Ne BE (kcal/mol)	16.12	14.92
close He BE (kcal/mol)	8.83	–
Δ close He BE (kcal/mol)	1.39	–
ω_1	1578.9	1581.2
$\Delta(\omega_1)$ (cm^{-1})	−62.4	−60.1
$\Delta(\nu_1)$ (cm^{-1})	−55.3	−53.4
f_1 (km/mol)	2019	2286
H–He Bond Length (Å)	0.953	2.328
H–Ne_1 Bond Length (Å)	1.117	1.142
H–Ne_2 Bond Length (Å)	2.331	1.141
H–$Ne_{3/4}$ Bond Length (Å)	3.384	2.478

barrier may be possible to observe this frequency, the fact that the He–H bond distance changes means that helium atom will likely reposition itself into structure c. before the vibrational signature of structure a. could be observed. Another possible phenomenon further limiting the lifetime of these species is the tunneling of neon atoms from one potential surface to another but is beyond the scope of the current work and will be left for future work.

3.4. $Ne_4He_2H^+$

Introduction of a second helium atom into the Ne_4HeH^+ structure was hoped to stabilize the He–H bonds. Instead, the same behavior seen in the single helium clusters is present. The short He–H bonds produce a minimum structure in structure a. from Fig. 6, but this is not the global minimum. The long He–H bonds with the helium atoms noncovalently interacting with the proton are preferred in structure b. In either case, only one helium atom bond length was varied in the scan, but the other mirrored it in the relaxed nature of this procedure even with symmetry reduced from D_{2h} to C_{2v}. A third isomer is also possible with the helium atoms adjacent to one another. However, the distant complexes for structure b. and the perpendicular He isomer (structure c.) are degenerate for the precision of the utilized CCSD(T)/aug-cc-pVTZ level of theory. Furthermore, the perpendicular He isomer actually reports an imaginary frequency of less than 15 cm^{-1} correlating with a bend that would put the helium atoms opposite one another creating structure b.

The vibrational frequencies of structure b. in Table 5 are in line with those from Ne_4HeH^+ implying that the additional noble gas atom in the shell does not greatly perturb the system. The frequency for structure a. is notably different from the corresponding isomer in Ne_4HeH^+, but structure a. for $Ne_4He_2H^+$ has helium atoms opposite one another raising the vibrational frequency above that for Ne_4HeH^+ where a helium and neon are opposite one another about the proton. In structure b. where the neon atoms are opposite one another, ω_1 is nearly identical to that for Ne_4HeH^+ further implying convergence of the first solvation shell.

4. Conclusions

HeH^+ cannot be stabilized in a shell of neon atoms. At best, it can produce the $NeHeH^+$ proton-bound complex, a molecule of its own interest, but not the first molecule in the universe, HeH^+. As more neon atoms are added to the complex, they assume the position of the two closest atoms to the proton, creating a proton-bound complex with noncovalently interacting atoms around it. This includes any helium atoms present along with any additional neon atoms. The helium atom can be relatively strongly bound to the central proton, but incident energies on the order of 2.5 kcal/mol will readily push the He–H bond to a point where it breaks replacing the helium with neon. The bright vibrational frequency found in proton-bound complexes begins to converge to 1580 cm^{-1} harmonically and likely close to 1398 cm^{-1} anharmonically as more neon atoms are added putting the experimental solvated frequency closer to 1350 cm^{-1} due to considerations from CcCR and experimental frequencies for this motion in He_2He^+ [23,26]. Hence, the presence of the helium atom is almost completely unfelt.

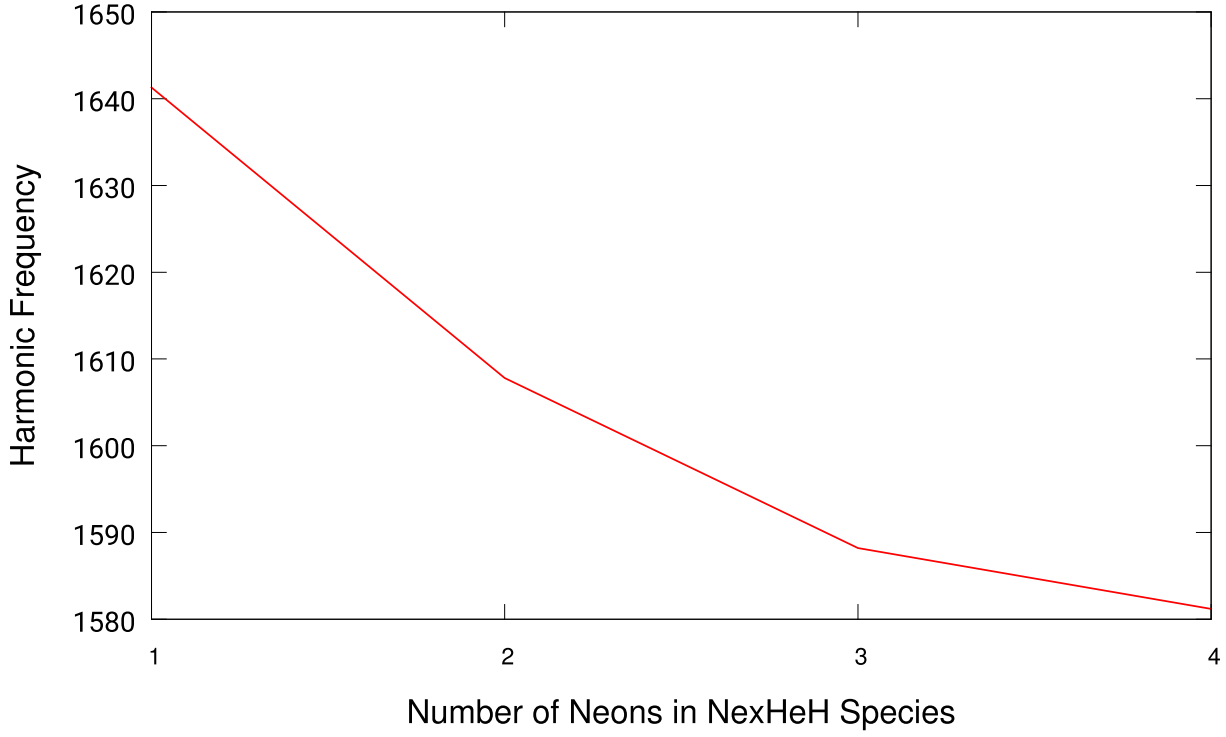

Fig. 5. The change in harmonic frequencies as the number of neons in the Ne_xHeH^+ species increases.

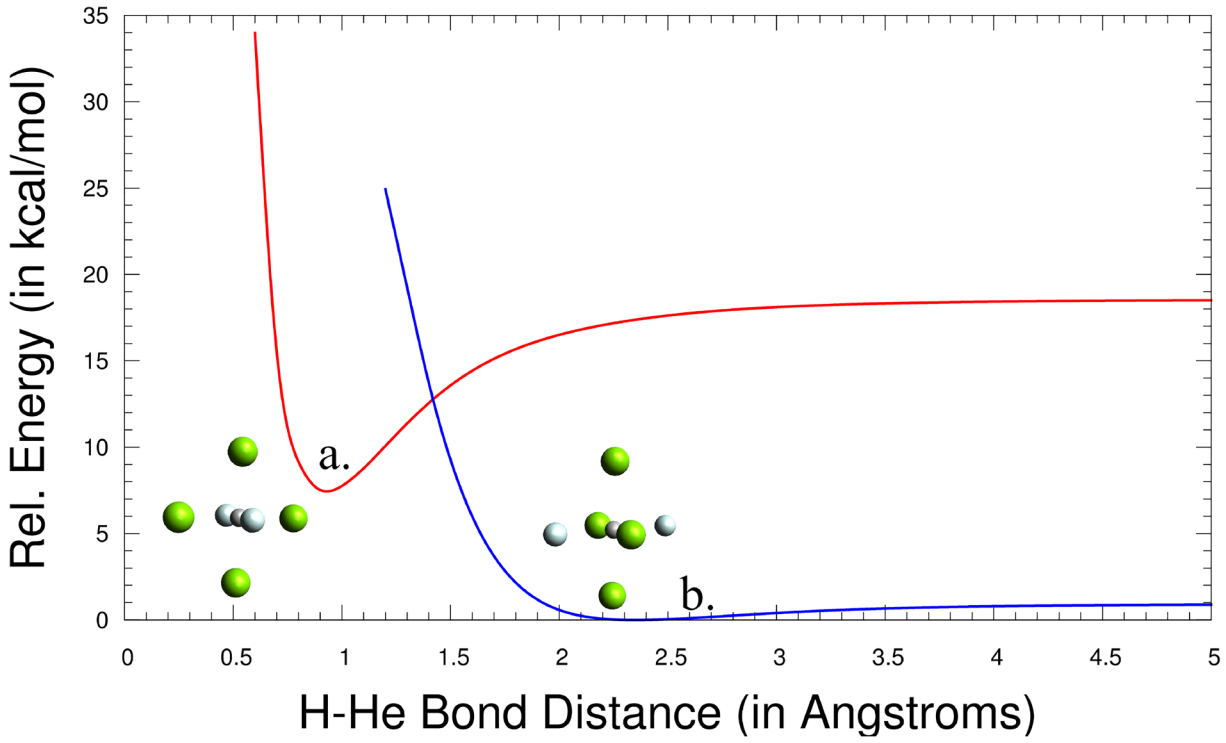

Fig. 6. The He–H dissociation PES for the two isomers of $Ne_4He_2H^+$: Structure a. in red and b. in blue.

Table 5
Optomized properties of Ne_4He_2H+.

	Structure a.	Structure b.	Structure c.
ΔE (kcal/mol)	8.74	0.00	0.00
distant He BE (kcal/mol)	–	0.53	0.57
distant Ne BE (kcal/mol)	1.57	1.26	1.37
close He BE (kcal/mol)	13.69	–	–
close Ne BE (kcal/mol)	–	14.43	14.45
ω_1	1644.0	1581.5	1584.2
f_1 (km/mol)	1735	2234	2234
H–He Bond Length (Å)	0.947	2.350	2.357
H–Ne_1 Bond Length (Å)	2.278	1.142	1.142
H–Ne_2 Bond Length (Å)	2.278	2.477	2.479

Again, mixed $NeHeH^+$ may yet be observed opening the door for potential observation of $OCHHe^+$ and N_2HHe^+, but once a third ligand is added, the helium will be retained in the system as a distant ligand at best. Most likely it will simply evaporate from the complex.

This behavior further showcases that HeH^+ is a rare molecule. Even solvated in the next-least reactive atom, neon, HeH^+ will dissociate the system with the slightest provocation. HeH^+ can only be studied in the gas phase (or theoretically), and even its proton-bound dimer, He_2H^+, will easily break apart upon exposure to any other atoms, again, even neon. Consequently, the early universe and the shells of supernova remnants are almost certainly the only places where HeH^+ and any of its derivatives are likely to be found in nature.

CRediT authorship contribution statement

Jax Dallas: Conceptualization, Data curation, Formal analysis, Investigation, Methodology, Software, Validation, Visualization, Writing - original draft, Writing - review & editing. **Athena Flint:** Conceptualization, Investigation, Methodology, Software, Visualization, Writing - original draft. **Ryan C. Fortenberry:** Conceptualization, Data curation, Formal analysis, Funding acquisition, Investigation, Project administration, Resources, Software, Supervision, Validation, Visualization, Writing - original draft, Writing - review & editing.

Declaration of Competing Interest

The authors declare that they have no known competing financial interests or personal relationships that could have appeared to influence the work reported in this paper.

Acknowledgements

The authors would like to acknowledge funding from NASA Grant NNX17AH15G, NSF Grant OIA-1757220, and from NSF Grant CHE-1757888. Additionally, JD would like to acknowledge support from The Barry Goldwater Scholarship and Excellence in Education Foundation.

References

[1] G. Frenking, D. Cremer, The chemistry of the noble gas elements helium, neon, and argon - experimental facts and theoretical predictions, Struct. Bond. 73 (1990) 17–95.
[2] H. Linnartz, D. Verdes, J.P. Maier, Rotationally resolved infrared spectrum of the charge transfer complex Ar-N_2^+, Science 297 (2002) 1166–1167.
[3] F. Grandinetti, Review: gas-phase ion chemistry of the noble gases: recent advances and future perspectives, Eur. J. Mass Spectrom. 17 (2011) 423–463.
[4] P. Bartl, C. Leidlmair, S. Denifl, P. Scheier, O. Echt, Cationic complexes of hydrogen with helium, Chem. Phys. Chem. 14 (2013) 227–232.
[5] S.J. Grabowski, J.M. Ugalde, D.M. Andrada, G. Frenking, Comparison of hydrogen and gold bonding in XHX^-, $XAuX^-$, and isoelectronic $NgHNg^+$, $NgAuNg^+$ (X = halogen, Ng = noble gas), Chem. Eur. J. 22 (2016) 11317–11328.
[6] R.A. Theis, R.C. Fortenberry, Potential interstellar noble gas molecules: $ArOH^+$ and $NeOH^+$ rovibrational analysis from quantum chemical quartic force fields, Mol. Astrophys. 2 (2016) 18–24.
[7] J.P. Wagner, D.C. McDonald II, M.A. Duncan, An argonoxygen covalent bond in the $ArOH^+$ molecular ion, Angew. Chem. Int. Ed. 57 (2018) 5081–5085.
[8] D. Galli, F. Palla, The dawn of chemistry, Ann. Rev. Astron. Astrophys. 51 (2013) 163–206.
[9] S. Bovino, M. Tacconi, F.A. Gianturco, D. Galli, Ion chemistry in the early universe: revisiting the role of HeH^+ with new quantum calculations, Astron. Astrophys. 529

(2011) A140.
[10] B.J. McCall, Dissociative recombination of cold H_3^+ and its interstellar implications, Philos. Trans. R. Soc. A 364 (2006) 2953–2963.
[11] O.L. Polyansky, A. Alijah, N.F. Zobov, I.I. Mizus, R.I. Ovsyannikov, J. Tennyson, L. Lodi, T. Szidarovszky, A.G. Császár, Spectroscopy of H_3^+ based on a new high-accuracy global potential energy surface, Philos. Trans. R. Soc. A 370 (2012) 5014–5027.
[12] R. Güsten, H. Wiesemeyer, D. Neufeld, K.M. Menten, U.U. Graf, K. Jacobs, B. Klein, O. Ricken, C. Risacher, J. Stutzki, Astrophysical detection of the helium hydride ion HeH^+, Nature 568 (2019) 357–359.
[13] I. Zinchenko, V. Dubrovich, C. Henkel, A search for HeH^+ and CH in a high-redshift quasi-stellar object, Mon. Not. R. Aston. Soc. 417 (2011) L76–L80.
[14] R.C. Fortenberry, The oldest molecular ancestor finally brought into the light, Chem 5 (2019) 1028–1030.
[15] T.R. Hogness, E.G. Lunn, The ionization of hydrogen by electron impact as interpreted by positive ray analysis, Phys. Rev. 26 (1925) 44–55.
[16] O. Novotný, P. Wilhelm, D. Paul, S. Ábel Kálosi, A. Saurabh, K. Becker, S. Blaum, J. George, M. Göck, F. Grieser, R. von Grussie, C. Hahn, H. Krantz, C. Kreckel, P.M. Meyer, D. Mishra, F. Muell, D.A. Nuesslein, M. Orlov, V.C. Rimmler, A. Schmidt, A.S. Shornikov, S. Terekhov, D. Vogel, A. Wolf Zajfman, Quantum-stateselective electron recombination studies suggest enhanced abundance of primordial HeH^+, Science 365 (2019) 676–679.
[17] M.A. Duncan, Infrared spectroscopy to probe structure and dynamics in metal ion-molecule complexes, Int. Rev. Phys. Chem. 22 (2003) 407–435.
[18] G.E. Douberly, R.S. Walters, J. Cui, K.D. Jordan, M.A. Duncan, Infrared spectroscopy of small protonated water clusters, $H^+(H_2O)_n$ (n = 2–5): isomers, argon tagging, and deuteration, J. Phys. Chem. A 114 (2010) 4570–4579.
[19] D.T. Mauney, J.D. Mosley, L.R. Madison, A.B. McCoy, M.A. Duncan, Infrared spectroscopy and theory of the formaldehyde cation and its hydroxymethylene isomer, J. Chem. Phys. 145 (2016) 174303 .
[20] R.A. Theis, R.C. Fortenberry, On the spectroscopic constants, first electronic state, vibrational frequencies, and isomerization of hydroxymethylene ($HCOH^+$), Mol. Astrophys. 8 (2017) 27–35.
[21] D.C. McDonald II, D.T. Mauney, D. Leicht, J.H. Marks, J.A. Tan, J.-L. Kuo, M.A. Duncan, Communication: trapping a proton in argon: spectroscopy and theory of the proton-bound argon dimer and its solvation, J. Chem. Phys. 145 (2016) 231101 .
[22] R.C. Fortenberry, Rovibrational characterization of the proton-bound, noble gas complexes: $ArHNe^+$, $ArHAr^+$, and $NeHNe^+$, ACS Earth Space Chem. 1 (2017) 60–69.
[23] C.J. Stephan, R.C. Fortenberry, The interstellar formation and spectra of the noble gas, proton-bound $HeHHe^+$, $HeHNe^+$ and $HeHAr^+$ complexes, Mon. Not. R. Astron. Soc. 469 (2017) 339–346.
[24] C.T. Bop, K. Hammami, N.A.B. Faye, Collisional rates based on the first potential energy surface of the NeH^+-He system, Mon. Not. R. Astron. Soc. 470 (2017) 2911–2917.
[25] A.G. Császár, T. Szidarovszky, O. Asvany, S. Schlemmer, Fingerprints of microscopic superfluidity in HHe+n clusters, Mol. Phys. 117 (2019) 1559–1583.
[26] O. Asvany, S. Schlemmer, T. Szidarovsky, A.G. Csaszar, Infrared signatures of the HHe_n^+ and DHe_n^+ (n = 3-6) complexes, J. Phys. Chem. Lett. 10 (2019) 5325–5330.
[27] D. Koner, L. Barrios, T. Gonzalez-Lezana, A.N. Panda, Wave packet and statistical quantum calculations for the He + $NeH^+ \rightarrow HeH^+$ + Ne reaction on the ground electronic state, J. Chem. Phys.
[28] B.D. Savage, K.R. Sembach, Interstellar abundances from absorption-line observations with the Hubble Space Telescope, Annu. Rev. Astron. Astrophys. 34 (1996) 279–329.
[29] K. Terrill, D.J. Nesbitt, ab initio anharmonic vibrational frequency predictions for linear proton-bound complexes OC-H+ -CO and N_2-H^+-N_2, Phys. Chem. Chem. Phys. 12 (2010) 8311–8322.
[30] R.C. Fortenberry, Q. Yu, J.S. Mancini, J.M. Bowman, T.J. Lee, T.D. Crawford, W.F. Klemperer, J.S. Francisco, Communication: Spectroscopic consequences of proton delocalization in $OCHCO^+$, J. Chem. Phys. 143 (2015) 071102 .
[31] Q. Yu, J.M. Bowman, R.C. Fortenberry, J.S. Mancini, T.J. Lee, T.D. Crawford, W. Klemperer, J.S. Francisco, The structure, anharmonic vibrational frequencies, and intensities of $NNHNN^+$, J. Phys. Chem. A 119 (2015) 11623–11631.
[32] R.C. Fortenberry, T.J. Lee, J.S. Francisco, Towards the astronomical detection of the proton-bound complex NN-HCO^+: implications for the spectra of protoplanetary disks, Astrophys. J. 819 (2016) 141.
[33] R.C. Fortenberry, T.J. Lee, J.S. Francisco, Quantum chemical analysis of the CO-HNN^+ proton-bound complex, J. Phys. Chem. A 120 (2016) 7745–7752.
[34] P. Gamallo, F. Huarte-Larrañaga, M. González, Resonances in the Ne + $H_2^+ \rightarrow$ NeH^+ + H proton-transfer reaction, J. Phys. Chem. A 117 (2013) 5393–5400.
[35] R.A. Theis, W.J. Morgan, R.C. Fortenberry, ArH_2^+ and NeH_2^+ as global minima in the Ar^+/Ne^+ + H_2 reactions: energetic, spectroscopic, and structural data, Mon. Not. R. Astron. Soc. 446 (2015) 195–204.
[36] A.C. Scheiner, G.E. Scuseria, J.E. Rice, T.J. Lee, H.F. Schaefer III, Analytic evaluation of energy gradients for the single and double excitation coupled cluster (ccsd) wave function: theory and application, J. Chem. Phys. 87 (7) (1987) 5361–5373.
[37] K. Raghavachari, G.W. Trucks, J.A. Pople, M. Head-Gordon, A fifth-order perturbation comparison of electron correlation theories, Chem. Phys. Lett. 157 (1989) 479–483.
[38] T.D. Crawford, H.F. Schaefer III, An introduction to coupled cluster theory for computational chemists, in: K.B. Lipkowitz, D.B. Boyd (Eds.), Reviews in Computational Chemistry, vol. 14, Wiley, New York, 2000, pp. 33–136.
[39] I. Shavitt, R.J. Bartlett, Many-Body Methods in Chemistry and Physics: MBPT and Coupled-Cluster Theory, Cambridge University Press, Cambridge, 2009.
[40] T.H. Dunning, Gaussian basis sets for use in correlated molecular calculations. I. The atoms boron through neon and hydrogen, J. Chem. Phys. 90 (1989) 1007–1023.
[41] R.A. Kendall, T.H. Dunning, R.J. Harrison, Electron affinities of the first-row atoms revisited. Systematic basis sets and wave functions, J. Chem. Phys. 96 (1992) 6796–6806.
[42] H.-J. Werner, P.J. Knowles, G. Knizia, F.R. Manby, M. Schütz, P. Celani, W. Györffy, D. Kats, T. Korona, R. Lindh, A. Mitrushenkov, G. Rauhut, K.R. Shamasundar, T.B. Adler, R.D. Amos, A. Bernhardsson, A. Berning, D.L. Cooper, M.J.O. Deegan, A.J. Dobbyn, F. Eckert, E. Goll, C. Hampel, A. Hesselmann, G. Hetzer, T. Hrenar, G. Jansen, C. Köppl, Y. Liu, A.W. Lloyd, R.A. Mata, A.J. May, S.J. McNicholas, W. Meyer, M.E. Mura, A. Nicklass, D.P. O'Neill, P. Palmieri, D. Peng, K. Pflüger, R. Pitzer, M. Reiher, T. Shiozaki, H. Stoll, A.J. Stone, R. Tarroni, T. Thorsteinsson, M. Wang, Molpro, version 2015.1, a package of ab initio programs, seehttp://www.molpro.net (2015).
[43] H.-J. Werner, P.J. Knowles, G. Knizia, F.R. Manby, M. Schütz, Molpro: a general-purpose quantum chemistry program package, WIREs Comput. Mol. Sci. 2 (2012) 242–253.
[44] G.F. Filipek II, R.C. Fortenberry, The formation of potential interstellar noble gas molecules in gas and adsorbed phases, ACS Omega 1 (2016) 765–772.
[45] C. Møller, M.S. Plesset, Note on an approximation treatment for many-electron systems, Phys. Rev. 46 (1934) 618–622.
[46] W.J. Hehre, R. Ditchfeld, J.A. Pople, Self-consistent molecular orbital methods. XII. Further extensions of gaussian-type basis sets for use in molecular orbital studies of organic molecules, J. Chem. Phys. 56 (1972) 2257.
[47] M.J. Frisch, G.W. Trucks, H.B. Schlegel, G.E. Scuseria, M.A. Robb, J.R. Cheeseman, G. Scalmani, V. Barone, B. Mennucci, G.A. Petersson, H. Nakatsuji, M. Caricato, X. Li, H.P. Hratchian, A.F. Izmaylov, J. Bloino, G. Zheng, J.L. Sonnenberg, M. Hada, M. Ehara, K. Toyota, R. Fukuda, J. Hasegawa, M. Ishida, T. Nakajima, Y. Honda, O. Kitao, H. Nakai, T. Vreven, J.A. Montgomery, Jr., J.E. Peralta, F. Ogliaro, M. Bearpark, J.J. Heyd, E. Brothers, K.N. Kudin, V.N. Staroverov, R. Kobayashi, J. Normand, K. Raghavachari, A. Rendell, J.C. Burant, S.S. Iyengar, J. Tomasi, M. Cossi, N. Rega, J.M. Millam, M. Klene, J.E. Knox, J.B. Cross, V. Bakken, C. Adamo, J. Jaramillo, R. Gomperts, R.E. Stratmann, O. Yazyev, A.J. Austin, R. Cammi, C. Pomelli, J.W. Ochterski, R.L. Martin, K. Morokuma, V.G. Zakrzewski, G.A. Voth, P. Salvador, J.J. Dannenberg, S. Dapprich, A.D. Daniels, O. Farkas, J.B. Foresman, J.V. Ortiz, J. Cioslowski, D.J. Fox, Gaussian 09 Revision D.01, Gaussian Inc., Wallingford CT (2009).
[48] X. Huang, T.J. Lee, A procedure for computing accurate ab initio) quartic force fields: application to HO_2^+ and H_2O, J. Chem. Phys. 129 (2008) 044312 .
[49] X. Huang, T.J. Lee, Accurate ab initio quartic force fields for NH_2^- and CCH- and rovibrational spectroscopic constants for their isotopologs, J. Chem. Phys. 131 (2009) 104301 .
[50] X. Huang, P.R. Taylor, T.J. Lee, Highly accurate quartic force field, vibrational frequencies, and spectroscopic constants for cyclic and linear $C_3H_3^+$, J. Phys. Chem. A 115 (2011) 5005–5016.
[51] R.C. Fortenberry, X. Huang, J.S. Francisco, T.D. Crawford, T.J. Lee, Quartic force field predictions of the fundamental vibrational frequencies and spectroscopic constants of the cations $HOCO^+$ and $DOCO^+$, J. Chem. Phys. 136 (2012) 234309 .
[52] X. Huang, R.C. Fortenberry, T.J. Lee, Spectroscopic constants and vibrational frequencies for *l*-C_3H^+ and isotopologues from highly-accurate quartic force fields: The detection of *l*-C_3H^+ in the horsehead nebula pdr questioned, Astrophys. J. Lett. 768 (2013) 25.
[53] D. Zhao, K.D. Doney, H. Linnartz, Laboratory gas-phase detection of the cyclopropenyl cation (c)-$C_3H_3^+$, Astrophys. J. Lett. 791 (2014) L28.
[54] R.C. Fortenberry, X. Huang, D.W. Schwenke, T.J. Lee, Limited rotational and rovibrational line lists computed with highly accurate quartic force fields and ab initio dipole surfaces, Spectrochim. Acta A 119 (2014) 76–83.
[55] R.C. Fortenberry, T.J. Lee, H.S.P. Müller, Excited vibrational level rotational constants for SiC_2: a sensitive molecular diagnostic for astrophysical conditions, Mol. Astrophys. 1 (2015) 13–19.
[56] M.J.R. Kitchens, R.C. Fortenberry, The rovibrational nature of closed-shell third-row triatomics: HOX and HXO, X = Si^+, P, S^+, and Cl, Chem. Phys. 472 (2016) 119–127.
[57] L. Bizzocchi, V. Lattanzi, J. Laas, S. Spezzano, B.M. Giuliano, D. Prudenzano, C. Endres, O. Sipilä, P. Caselli, Accurate sub-millimetre rest frequencies for $HOCO^+$ and $DOCO^+$ ions, Astron. Astrophys. 602 (2017) A34.